A Common Mechanism Underlying Promiscuous Inhibitors from Virtual and High-Throughput Screening

Susan L. McGovern,[‡] Emilia Caselli,[‡,§] Nikolaus Grigorieff,[⊥] and Brian K. Shoichet*[,‡]

Department of Molecular Pharmacology and Biological Chemistry, Northwestern University, 303 East Chicago Avenue, Chicago, Illinois 60611, and Howard Hughes Medical Institute, W. M. Keck Institute for Cellular Visualization, Rosenstiel Basic Medical Research Center, Brandeis University, 415 South Street, Waltham, Massachusetts 02454

Received November 20, 2001

High-throughput and virtual screening are widely used to discover novel leads for drug design. On examination, many screening hits appear non-drug-like: they act noncompetitively, show little relationship between structure and activity, and have poor selectivity. Attempts to develop these peculiar molecules into viable leads are often futile, and much time can be wasted on the characterization of these "phony" hits. Despite their common occurrence, the mechanism of action of these promiscuous molecules remains unknown. To investigate this problem, 45 diverse screening hits were studied. Fifteen of these were previously reported as inhibitors of various receptors, including β-lactamase, malarial protease, dihydrofolate reductase, HIV Tar RNA, thymidylate synthase, kinesin, insulin receptor, tyrosine kinases, farnesyltransferase, gyrase, prions, triosephosphate isomerase, nitric oxide synthase, phosphoinositide 3-kinase, and integrase; 30 were from an in-house screening library of a major pharmaceutical company. In addition to their original targets, 35 of these 45 compounds were shown to inhibit several unrelated model enzymes. These 35 screening hits included compounds, such as fullerenes, dyes, and quercetin, that have repeatedly shown activity against diverse targets. When tested against the model enzymes, the compounds showed time-dependent but reversible inhibition that was dramatically attenuated by albumin, guanidinium, or urea. Surprisingly, increasing the concentration of the model enzymes 10-fold largely eliminated inhibition, despite a 1000-fold excess of inhibitor; a well-behaved competitive inhibitor did not show this behavior. One model to explain these observations was that the active form of the promiscuous inhibitors was an aggregate of many individual molecules. To test this hypothesis, light scattering and electron microscopy experiments were performed. The nonspecific inhibitors were observed to form particles of 30−400 nm diameter by both techniques. In control experiments, a well-behaved competitive inhibitor and an inactive dye-like molecule were not observed to form aggregates. Consistent with the hypothesis that the aggregates are the inhibitory species, the particle size and IC_{50} values of the promiscuous inhibitors varied monotonically with ionic strength; a competitive inhibitor was unaffected by changes in ionic strength. Unexpectedly, aggregate formation appears to explain the activity of many nonspecific inhibitors and may account for the activity of many promiscuous screening hits. Molecules acting via this mechanism may be widespread in drug discovery screening databases. Recognition of these compounds may improve screening results in many areas of pharmaceutical interest.

Introduction

High-throughput and virtual screening are widely used to discover new lead compounds for drug design.[1−4] These screening methods have discovered novel molecules, dissimilar to known ligands, that nevertheless bind to the target receptor at micromolar or submicromolar concentrations.[5−8] Often, screening hits are subsequently found to have peculiar inhibition properties: they act noncompetitively, show little relationship between structure and activity, and have poor specificity.[9,10] These traits are non-drug-like and are undesirable in lead compounds. Accordingly, many attempts have been made to identify and remove molecules with these properties from screening databases.[11−13] Such efforts have not been entirely successful because the underlying causes of these unusual behaviors are not completely understood. Consequently, screening hit lists continue to be populated, even dominated, by compounds that act with atypical properties that cannot be described by any existing model; such compounds are unlikely to be pharmaceutically useful.

To determine the source of some of the peculiar properties observed with many screening hits, we initially investigated 15 diverse compounds derived from the literature and from our own unpublished work. All of these compounds were originally described as inhibitors of one or more proteins or nucleic acids. Regardless of their original targets or discovery method, we found that these screening hits also inhibited several unrelated model enzymes in a time-dependent and reversible manner. Based on kinetic and physical experiments, we

* To whom correspondence should be addressed. Tel: 312-503-0081. Fax: 312-503-5349. E-mail: b-shoichet@northwestern.edu.
‡ Northwestern University.
⊥ Brandeis University.
§ Present address: Dipartimento di Chimica, Università degli Studi di Modena, Via Campi 183, Modena, Italy.

10.1021/jm010533y CCC: $22.00 © 2002 American Chemical Society
Published on Web 03/09/2002

Table 1. Nonspecific Inhibitors Discovered by Screening

Structure	Original Target(s)		IC_{50} (μM) β-lactamase	Chymotrypsin	cDHFR	β-gal
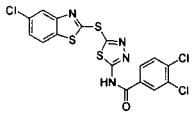	0.5 β-lactamase[a]		0.5	2.5	5	15
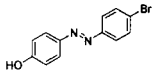	5 β-lactamase[a]		5	25	35	90
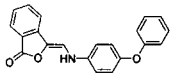	5 β-lactamase[a]		5	15	N.D.	N.D.
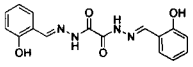	8 malarial protease[14]		10	55	70	180
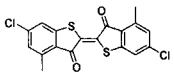	7 pDHFR[15]		10	50	60	300
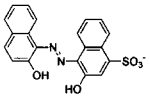	80 pDHFR[15]		50	25	N.D.	600
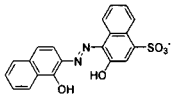	50 HIV Tar RNA[16]		10	90	N.D.	600
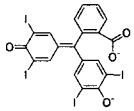	3 TS[8]	30 kinesin[17]	3	11	20	200
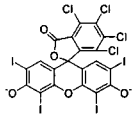	20[b] insulin receptor[18]	7.5 kinesin[17]	16	50	N.D.	80
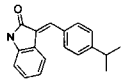	5.2 VEGF[9]	10.0 IGF-1[9]	6	30	30	55
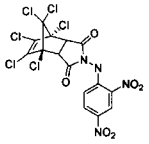	25 farnesyltransferase[19]		3	9	25	150
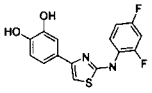	15[c] gyrase[10]		18	100	150	320
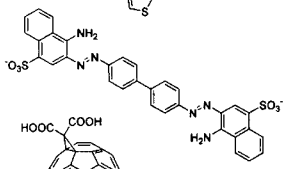	1 prion[20]	30.4 TIM[21]	3.9	40	0.4	100
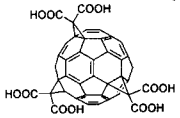	17 eNOS[22]	24 nNOS[22]	7	60	N.D.	N.D.
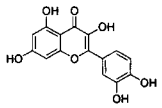	3.8 PI3K[23,24]	11.0 integrase[25]	4	100	N.D.	220

[a] Our unpublished observations. [b] K_d. [c] Maximal noneffective concentration. cDHFR, chicken DHFR; β-gal, β-galactosidase; pDHFR, *Pneumocystis carinii* DHFR; TS, thymidylate synthase; VEGF, vascular endothelial growth factor receptor tyrosine kinase; IGF-1, insulin-like growth factor receptor tyrosine kinase; TIM, triosephosphate isomerase; eNOS, endothelial nitric oxide synthase; nNOS, neuronal nitric oxide synthase; PI3K, phosphoinositide 3-kinase; N.D., not determined.

Table 2. Effect of Incubation or a 10-Fold Increase in Enzyme Concentration on Inhibition of β-Lactamase

Structure	↓ IC_{50} with Incubation	↑ IC_{50} vs. 10x Enzyme	Structure	↓ IC_{50} with Incubation	↑ IC_{50} vs. 10x Enzyme
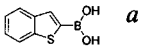 *a*	No change	No change	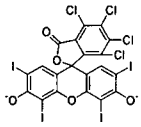	3-fold	22-fold
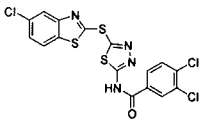	6-fold	7-fold			
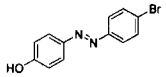	23-fold	23-fold	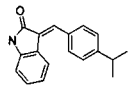	> 50-fold	> 50-fold
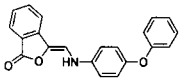	4-fold	40-fold	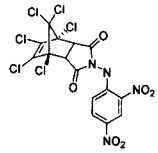	44-fold	22-fold
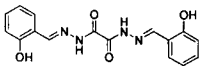	22-fold	40-fold	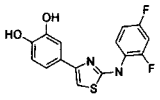	9-fold	7-fold
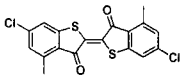	32-fold	6-fold	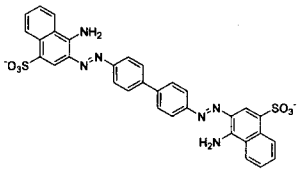	11-fold	15-fold
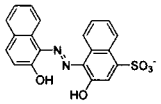	6-fold	7-fold			
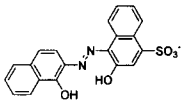	3-fold	4-fold	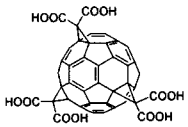	2-fold	> 50-fold
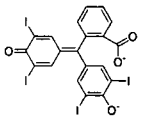	7-fold	> 50-fold	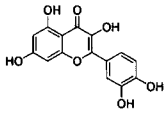	2-fold	> 50-fold

[a] Benzo[*b*]thiophene-2-boronic acid, a specific, competitive, and reversible inhibitor of AmpC β-lactamase.[26]

propose a simple biophysical mechanism to account for this behavior. Subsequent experiments indicate that compounds acting via this mechanism exist in the screening library of a major pharmaceutical company; such nonspecific inhibitors may be widespread in drug discovery databases.

Results and Discussion

To investigate the unusual, non-drug-like behavior displayed by many screening hits, we first studied 15 small-molecule inhibitors discovered by screening (Table 1). These compounds came from multiple virtual and high-throughput screening projects against a variety of targets,[8−10,14−25] including functionally and structurally diverse enzymes, an RNA segment, and a prion. Regardless of the particular target that each compound was initially shown to inhibit, we found that these 15 molecules were micromolar inhibitors of several unrelated model enzymes, including β-lactamase, chymotrypsin, dihydrofolate reductase (DHFR), and β-galactosidase.

Inhibition by these compounds was time-dependent (Table 2). When inhibitor and β-lactamase were preincubated, the IC_{50} decreased (improved) 2- to over 50-fold compared to the IC_{50} when enzyme and inhibitor were not preincubated. A well-studied competitive inhibitor of β-lactamase was not affected by incubation.[26]

Many time-dependent, nonspecific inhibitors are thought to form irreversible enzyme adducts.[27] One test for irreversible binding is to incubate the inhibitor and enzyme at high concentrations and then to dilute the incubation mixture to below the apparent IC_{50} of the inhibitor. When this was done with β-lactamase and moxalactam, a known irreversible β-lactamase inhibitor,[28] the enzyme remained fully inhibited upon dilution, as expected. When the same test was performed with the screening hits, full enzyme activity returned after dilution (data not shown). This suggested that inhibition by these nonspecific inhibitors was reversible and did not occur via a covalent adduct.

Another mechanism of nonspecific inhibition is denaturation.[29] If these screening hits acted as denaturants, their potency should increase with temperature or with the concentration of solvent denaturants such as urea or guanidinium. However, temperature had little effect on inhibition (data not shown), and guanidinium or urea either did not affect or actually *reduced*

Table 3. Effect of Guanidinium, Urea, or BSA on Inhibition of β-Lactamase, β-Galactosidase, or Chymotrypsin

Structure	↑ IC_{50} in the presence of GndHCl	Urea	BSA
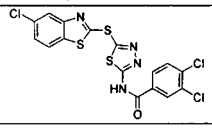	3-fold	No effect	> 50-fold[a] > 50-fold[b] > 50-fold[c]
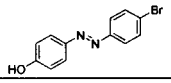	6-fold	2-fold	8-fold[b] 18-fold[c]
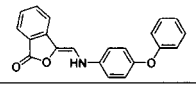	3-fold	7-fold	> 50-fold[a] 9-fold[b] 12-fold[c]
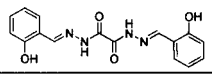	6-fold	4-fold	> 50-fold[a] 4-fold[c]
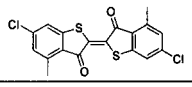	19-fold	3-fold	12-fold[a] 6-fold[c]
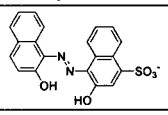	4-fold	N.D.	> 50-fold[a] > 50-fold[c]

All guanidinium and urea data were obtained against β-lactamase. [a] Against β-lactamase. [b] Against β-galactosidase. [c] Against chymotrypsin. N.D., not determined.

inhibition by 2- to 19-fold (Table 3). This seemed inconsistent with a denaturant mechanism of inhibition.

Nonspecific binding is often detected by decreased inhibition in the presence of bovine serum albumin (BSA). Inhibition of β-lactamase, β-galactosidase, or chymotrypsin by six screening hits decreased 4- to over 50-fold in the presence of 0.1 mg/mL BSA (Table 3). These results supported a nonspecific mechanism for these compounds and suggested that inhibition by these molecules might be attenuated by the presence of excess protein.

In fact, the first suggestion of a unifying mechanism followed the discovery that the IC_{50} values of all compounds increased (worsened) 4- to over 50-fold when the concentration of one of the model enzymes, β-lactamase, was increased 10-fold, from 1 nM to 10 nM (Table 2). A competitive, reversible inhibitor of β-lactamase was unaffected by the increase in enzyme, consistent with the assumption that an enzyme present at nanomolar concentrations would not significantly affect the free concentration of a well-behaved inhibitor present at micromolar concentrations. All compounds tested for this effect also showed an increase in IC_{50} against chymotrypsin when the concentration of this enzyme was increased 10-fold (data not shown). To account for the extreme sensitivity of these screening hits to the molar ratio of inhibitor to enzyme, we considered the hypothesis that the active inhibitor might be an aggregate of many individual molecules.

To determine if these compounds formed aggregates in water, dynamic light scattering (DLS) was initially performed on aqueous mixtures of nine screening hits (Table 4) and subsequently on 20 other compounds (Table 6). For all of these compounds, the presence of submicron particles with strong scattering intensity was suggested by the large amplitude of the autocorrelation function at the smallest values of τ and by the decay of the autocorrelation function over the 10−1000 μs time

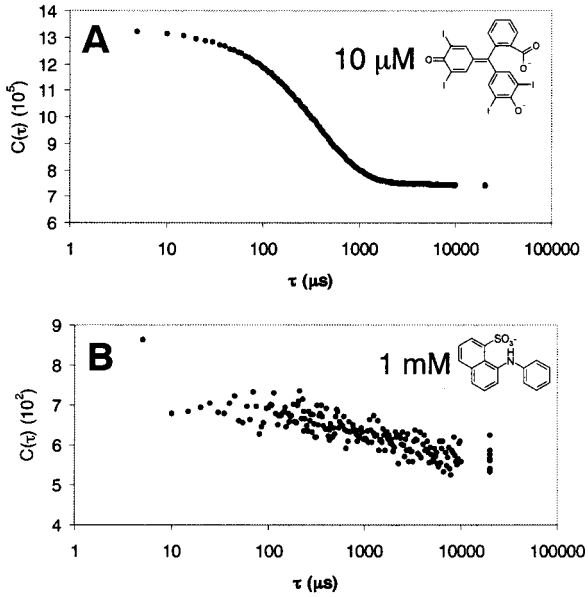

Figure 1. Representative autocorrelation functions from dynamic light scattering: (A) 10 μM tetraiodophenolphthalein in 50 mM KP_i; (B) 1 mM ANS in 50 mM KP_i. The laser power and integration times for the experiments in A and B are comparable.

scale (Figure 1A). This was also reflected in the intensity of the scattered light from these compounds: all showed scattering intensities at least an order of magnitude higher than buffer alone (Table 4). The apparent diameter of the particles varied from 95 to 400 nm, depending on the compound. These particles dwarf β-lactamase, DHFR, chymotrypsin, and β-galactosidase, which are 6.5, 5.0, 5.4, and 18.5 nm, respectively, in their longest dimensions. In control experiments, 8-anilino-1-naphthalene-sulfonic acid (ANS), a dye that is structurally similar to many of the nonspecific inhibitors but does not inhibit the model enzymes and does not assemble into aggregates,[30] yielded a low amplitude

Table 4. Dynamic Light Scattering Reveals That Several Nonspecific Inhibitors Form Particles

Structure	IC_{50} vs. β-lactamase (μM)	DLS conc. (μM)	Intensity (kcps)	Diameter (nm)
50 mM KP_i	---	---	0.4 ± 0.1	No particles
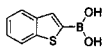 *a*	0.2	100	0.9 ± 0.2	No particles
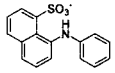 *b*	> 1600	1000	0.5 ± 0.1	No particles
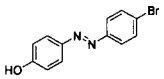	5	10	12.6 ± 3.9	176.2 ± 7.9
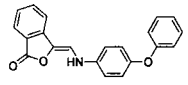	5	100	16.2 ± 1.1	94.7 ± 4.2
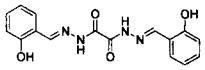	10	10	26.4 ± 5.1	394.6 ± 12.5
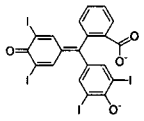	3	10	42.2 ± 3.9	153.4 ± 26.0
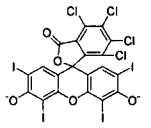 *c*	16	500	115.1 ± 65.6	403.1 ± 82.2
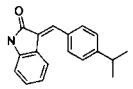	6	10	43.8 ± 5.7	379.0 ± 14.1
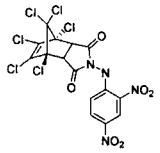	3	15	24.9 ± 3.1	418.6 ± 38.8
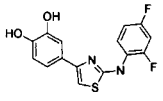	18	300	32.3 ± 4.3	165.1 ± 10.9
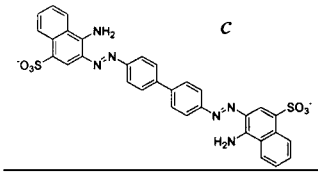 *c*	3.9	750	131.1 ± 64.3	202.6 ± 22.5

DLS performed in 50 mM KP_i at the concentration given under "DLS conc.". [a] A specific, competitive, and reversible inhibitor of AmpC β-lactamase.[26] [b] ANS is known not to aggregate.[30] [c] Compounds analyzed by DLS at 632.8 nm; all others analyzed at 514.4 nm. kcps, kilocounts per second.

autocorrelation function that lacked a well-defined decay, suggesting that it did not form particles in solution (Figure 1B and Table 4). Benzo[*b*]thiophene-2-boronic acid, a competitive inhibitor of β-lactamase, was also not observed to form particles (Table 4). Our positive control, Congo Red, a dye that has been shown to aggregate in solution[30] and that we found to inhibit the model enzymes (Table 1), did form particles detectable by DLS (Table 4).

Aggregates, such as micelles or vesicles, should be affected by ionic strength.[31] The nonspecific inhibitors decreased in potency by 1 to 2 orders of magnitude

Table 5. Effect of Ionic Strength on Inhibition and Aggregate Size

Structure	IC_{50} vs. β-lactamase (μM)			Diameter (nm) [a]		
	5mM KP_i	50mM KP_i	500mM KP_i	5mM KP_i	50mM KP_i	500mM KP_i
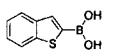 *b*	0.2	0.2	0.3	No particles	No particles	No particles
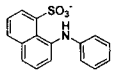	> 1600	> 1600	> 1600	No particles	No particles	No particles
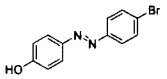	2.3	5	12	140.2 ± 12.1	176.2 ± 7.9	267.4 ± 24.5
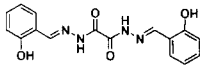	4	10	15	389.3 ± 55.4	394.6 ± 12.5	426.6 ± 23.8
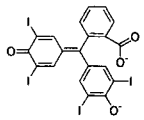	1	3	5	86.2 ± 10.5	153.4 ± 26.0	320.4 ± 38.8
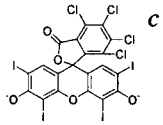 *c*	0.47	16	19	N.D.	403.1 ± 82.2	N.D.
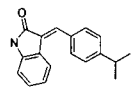	3	6	7	247.1 ± 12.8	379.0 ± 14.1	494.3 ± 48.1
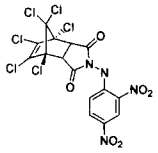	0.5	3	6	143.5 ± 7.9	418.6 ± 38.8	N.D.
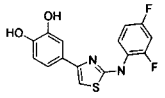	3	18	133	102.9 ± 9.9	165.1 ± 10.9	436.2 ± 24.8
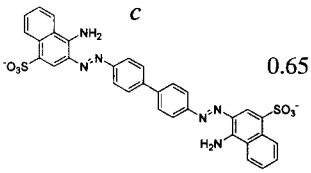 *c*	0.65	3.9	340	N.D.	202.6 ± 22.5	N.D.

[a] DLS experiments performed in 5, 50, or 500 mM KP_i at the concentration specified in Table 4. [b] A specific, competitive, and reversible inhibitor of AmpC β-lactamase.[26] [c] Compounds analyzed by DLS at 632.8 nm; all others analyzed at 514.4 nm. N.D., not determined.

against β-lactamase as the concentration of buffer was increased from 5 to 500 mM potassium phosphate (KP_i) (Table 5). Concomitantly, the mean diameter of the particles formed by these compounds monotonically increased with the ionic strength (Table 5). The potency of a competitive and reversible inhibitor did not change, suggesting that the changes in ionic strength did not significantly affect the enzyme.

The large size of the aggregates suggested that dialysis membranes would impede them. To investigate this prediction, the screening hits were individually incubated with β-lactamase at a high inhibitor concentration and dialyzed against buffer. As a control, a known reversible and specific inhibitor of β-lactamase was also incubated with the enzyme and dialyzed under the same conditions. Enzyme incubated with the reversible and specific inhibitor recovered full activity after dialysis—the inhibitor had equilibrated with the surrounding solution. Conversely, enzyme incubated with nonspecific inhibitors remained fully inhibited (data not shown). Although dilution experiments suggested that inhibition by these nonspecific inhibitors was reversible, inhibition was irreversible by equilibration through dialysis, consistent with the aggregation model.

If these nonspecific inhibitors form aggregates on the 100 nm scale, they should be visible by direct methods. We used transmission electron microscopy (TEM) to visualize the particles formed by two nonspecific inhibi-

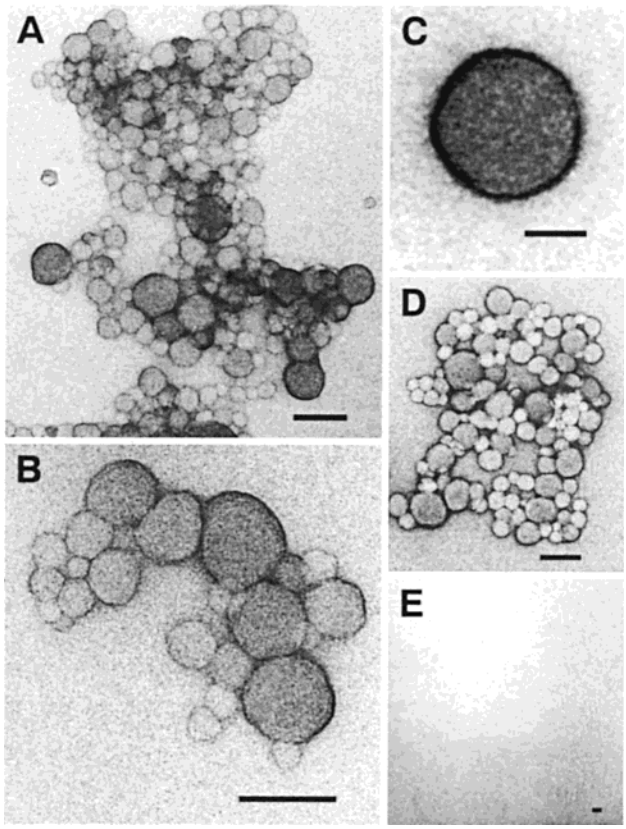

Figure 2. Compounds visualized by transmission electron microscopy: (A−C) 100 μM tetraiodophenolphthalein in 20 mM Tris; (D) 50 μM Congo Red in 20 mM Tris; (E) 625 μM ANS in 20 mM Tris. Bar = 100 nm.

tors, tetraiodophenolphthalein and Congo Red. Spherical aggregates ranging from 30 to 200 nm in diameter were observed in solutions of these compounds (Figure 2A−D), consistent with results from DLS on tetraiodophenolphthalein in the same conditions (mean diameter of 83.2 ± 6.5 nm). Analogues of the fullerene in Table 1 have also been shown to form spherical vesicles by TEM.[32] Particles were not observed in a solution of the negative control, ANS (Figure 2E), also consistent with results from DLS.

To determine if aggregate-forming nonspecific inhibitors are found in pharmaceutical high-throughput screening databases, 30 compounds from the screening library of Pharmacia Corporation were tested (Table 6). These compounds were biased toward molecules that hit in multiple screens against different targets. Of these 30 compounds, 20 inhibited β-lactamase and chymotrypsin with micromolar IC_{50} values. Similar to the nonspecific screening hits described above, inhibition by these pharmaceutical compounds improved when they were incubated with β-lactamase and worsened when the β-lactamase concentration was increased 10-fold. These inhibitors also formed strongly scattering particles detectable by DLS at micromolar concentrations (Table 6). These results suggest that molecules that inhibit enzymes by forming aggregates at micromolar concentrations may be common in pharmaceutical screening databases; such compounds would artificially raise hit rates in high-throughput screens for new drug leads.

An aggregation model (Figure 3) is surprising for several reasons, not least because it suggests a single mechanism of action for a diverse group of molecules. Nevertheless, it can be reconciled with the peculiar behavior of many promiscuous inhibitors. An aggregate could interact with many enzymes, accounting for the lack of specificity of these inhibitors. Similarly, an aggregate-based mechanism would explain the flat structure−activity relationships often observed with promiscuous inhibitors. Several factors could result in time-dependent inhibition, including formation of the aggregate, its interaction with the enzyme, and the low concentrations of both aggregate and enzyme. An aggregate could form reversibly and interact reversibly with enzyme; dilution would decrease the aggregate concentration and return active enzyme.

Inhibition by an aggregate species would also be extremely sensitive to the concentration of enzyme. Although the molar ratio of inhibitor to enzyme is roughly 10000:1 in these experiments, the ratio of aggregate particles to enzyme molecules will be much lower. Because of this low ratio, increasing the enzyme 10-fold might easily overwhelm the ability of the aggregate to inhibit the enzyme.

Direct physical measurements also support this model. DLS suggests that these compounds form 65−400 nm particles at concentrations similar to their IC_{50} values against the model enzymes. These particles increase in apparent size as the ionic strength increases, which should increase the number of monomers in each aggregate[31] but decrease the concentration of the aggregate, which is the inhibitory species. Thus, at higher ionic strength, more compound would be necessary to inhibit the enzyme. This ionic strength effect may also explain the effect of guanidinium on inhibition. Particles in the 100 nm range would also not be expected to passively diffuse through a 10 kDa dialysis membrane. Finally, the model is supported by our TEM observations that two nonspecific inhibitors form spherical aggregates in solution.

Several important questions remain unanswered by this work. For instance, what is the arrangement of molecules inside the aggregates? The compounds studied here do not resemble molecules typically found in micelles or vesicles, such as charged lipids. Instead,

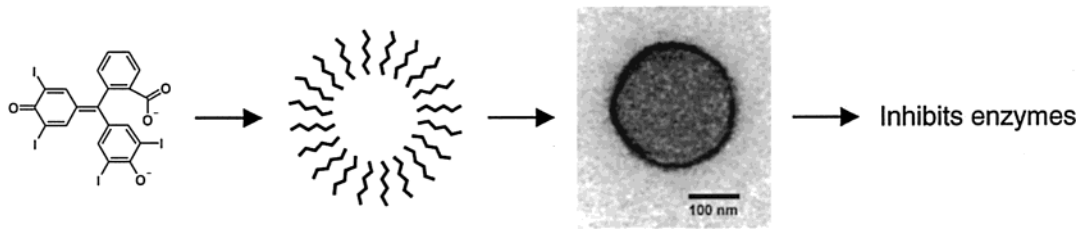

Figure 3. Summary of the proposed mechanism of nonspecific inhibition. Some small molecules form particles from 50 to over 400 nm in diameter, and these particles adsorb or absorb target enzymes, thereby inhibiting them.

Table 6. Nonspecific Inhibition and Aggregation by Compounds from the Pharmacia Screening Library

Structure	IC_{50} vs. β-lactamase (μM)	↓ IC_{50} with Incubation	↑ IC_{50} vs. 10x β-lactamase	IC_{50} vs. chymo. (μM)	DLS Conc. (μM)	DLS Intensity (kcps)	DLS Diameter (nm)
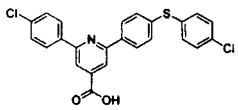	2	12-fold	4-fold	2	50	54.3 ± 5.5	100.4 ± 5.1
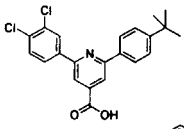	4	> 50-fold	12-fold	13	50	24.4 ± 2.6	97.1 ± 2.5
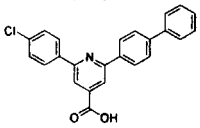	5	35-fold	10-fold	8	80[a]	19.2 ± 4.7	171.8 ± 35.8
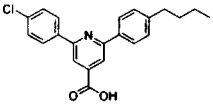	8	24-fold	20-fold	15	50	11.1 ± 2.4	106.9 ± 6.3
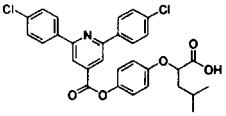	15	> 50-fold	5-fold	3	50	30.4 ± 2.5	108.5 ± 5.1
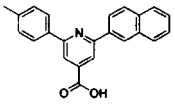	50	> 50-fold	4-fold	50	500[a]	13.5 ± 3.4	201.2 ± 44.4
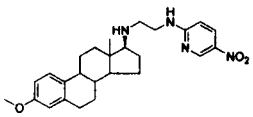	5	14-fold	> 50-fold	13	40[a]	20.2 ± 0.8	381.0 ± 30.4
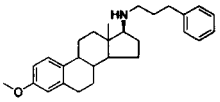	5	> 50-fold	> 50-fold	200	100	8.0 ± 0.6	297.4 ± 19.9
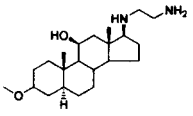	10	4-fold	4-fold	40	100	10.0 ± 1.9	N.D.
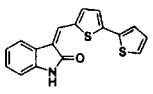	2	13-fold	8-fold	15	20	12.6 ± 4.3	N.D.
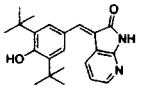	4	> 50-fold	6-fold	10	10[a]	14.2 ± 1.1	140.9 ± 9.0
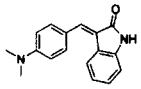	10	> 50-fold	3-fold	30	30[a]	51.2 ± 7.2	288.6 ± 21.8
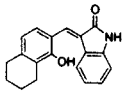	15	3-fold	6-fold	40	40	14.0 ± 5.9	N.D.
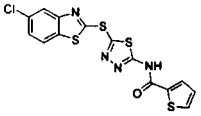	2	> 50-fold	3-fold	15	15	17.5 ± 1.8	172.5 ± 9.2

Table 6 (Continued)

Structure	IC_{50} vs. β-lactamase (μM)	↓ IC_{50} with Incubation	↑ IC_{50} vs. 10x β-lactamase	IC_{50} vs. chymo. (μM)	DLS Conc. (μM)	DLS Intensity (kcps)	DLS Diameter (nm)
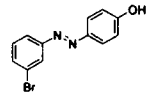	15	5-fold	> 50-fold	220	500	10.5 ± 2.5	184.4 ± 25.6
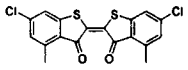	3	15-fold	3-fold	15	20	10.0 ± 0.3	205.8 ± 5.7
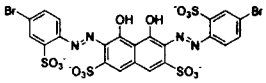	80	2-fold	> 50-fold	110	---[b]	---[b]	---[b]
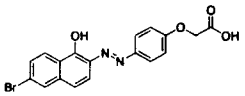	30	> 50-fold	8-fold	80	20	19.6 ± 2.7	N.D.
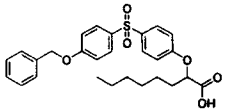	3	7-fold	9-fold	13	500[a]	3.0 ± 0.4	68.2 ± 7.6
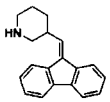	200	2-fold	> 50-fold	700	100	16.7 ± 1.2	221.0 ± 4.2

[a] DLS experiments in 5 mM KP_i; all others in 50 mM KP_i. [b] Compound absorbs significantly at 514.4 nm. Laser power was comparable in all experiments. chymo., chymotrypsin; N.D., not determined.

these screening hits are typically hydrophobic, planar, and rigid, with a few decorative polar groups. Preliminary ideas may be found in studies on Congo Red by Skowronek et al.[33] They suggest that the dye can self-assemble into highly ordered complexes, driven by stacking of the aromatic rings. A related model is proposed by Auweter et al. for the formation of spherical nanoparticles by β-carotene.[34] Their results suggest that β-carotene forms crystallites with an aggregation number on the order of 10 000 molecules. They propose that several "crystallites" associate to form the particle core, which is roughly 120 nm in diameter. Such models provide some initial hypotheses about the nature of the interactions involved in aggregate formation by screening hits and may allow one to set some bounds on the number of monomers in a 65−400 nm particle. Such limits should be considered preliminary as this remains an area of ongoing research.

We also do not know exactly how these aggregates inhibit their target enzymes. At least two models may be considered: enzyme molecules might be adsorbed to the surface of the aggregate, or enzyme molecules might be absorbed into the interior of the aggregate. Understanding this interaction is another area of ongoing research. These ambiguities should not obscure the key observation of this study that the active inhibitor species for many nonspecific screening hits is an aggregate of many individual molecules.

We have put no effort into developing a computational model for predicting compounds that act via an aggregation mechanism. Because we understand that such a model would be useful for the community, we have included the structures of the nonspecific inhibitors in .sdf format as Supporting Information so that others can develop their own models, should they wish to do so. It has not escaped our notice that experimental or even high-throughput methods might also be developed to identify these promiscuous compounds.

Aggregate-forming inhibitors may be found among both virtual and experimental screening hit lists (Table 1) and are well-represented in the literature.[8−10,14−25] These include results from several different computational screening algorithms, as well as hits from both enzyme-based and whole-cell high-throughput assays. Additionally, the results in Table 6 suggest that these compounds may be common in pharmaceutical screening libraries; such nonspecific inhibitors would artificially inflate hit rates in screening for new drug leads. Much effort can be wasted chasing aggregate forming "inhibitors" that are unlikely to be useful biologically. By understanding their mechanism of inhibition, these molecules can be identified rapidly and discarded in favor of classically behaved specific inhibitors.

Experimental Section

Materials. AmpC β-lactamase was purified as described.[26] Chymotrypsin, chicken liver DHFR, β-galactosidase, cephalothin, *N*-benzoyl-L-tyrosine-ethyl ester (BTEE), succinyl-ala-ala-pro-phe-*p*-nitroanilide, reduced β-nicotinamide adenine dinucleotide phosphate (NADPH), dihydrofolic acid (DHF), *O*-nitrophenyl-β-D-galactopyranoside (ONPG), oxalic-acid-bis-(salicylaldehyde hydrazide), 4-(4-bromophenylazo)phenol, hexachloro-4-(2,4-dinitro-phenylamino)-4-aza-tricyclo(5.2.1.0-(2,6))dec-ene-dione, tetraiodophenolphthalein, moxalactam, Congo Red, Rose Bengal lactone, palatine chrome black, and quercetin were purchased from Sigma-Aldrich. Cephalothin-G-ester was a gift from Eli Lilly. *N*1-[5-[(5-chloro-1,3-benzothiazol-2-yl)]-1,3,4-thiadiazol-2-yl]-3,4-dichloro and 3-(4-isopropylbenzylidene)indolin-2-one were purchased from May-

bridge Chemical; ANS and Vat Red I from TCI. (4-((2,4-Difluorophenyl)amino)-3,5-thiazolyl)benzene-1,2-diol was purchased from Menai Organics; 3-[(4-phenoxyanilino)methylene]-2-benzofuran-1(3*H*)-one from Bionet; benzo[*b*]thiophene-2-boronic acid from Lancaster Synthesis; nitrocefin from Oxoid; and tris(dicarboxymethylene)fullerene-C3 from Alexis Biochemicals. BSA was purchased from Calbiochem, guanidinium HCl from Amresco, and urea from Fisher Scientific. All materials were used as supplied by the manufacturer, without further purification.

Molecular Docking. A subset of the 1995/2 Available Chemicals Directory containing 153 536 molecules was docked against the structure of AmpC β-lactamase[35] with the Northwestern version of DOCK3.5 as described.[36]

Enzyme Assays. Compounds were tested for inhibition of β-lactamase, chymotrypsin, DHFR, and β-galactosidase. Unless otherwise stated, assays were performed in 50 mM KP_i buffer, pH 7.0 at 25 °C. Stocks of substrates and inhibitors were generally prepared at 10 mM in dimethyl sulfoxide (DMSO). No more than 6% DMSO was present in any assay, and results were controlled for the effect of DMSO. All reactions were monitored on an HP8453 spectrophotometer.

For most β-lactamase assays, inhibitor and 1 nM enzyme were incubated for 5 min, and the reaction was initiated with 100 μM cephalothin[26] or 200 μM nitrocefin. For β-lactamase assays without incubation, inhibitor and 100 μM cephalothin or 200 μM nitrocefin were mixed, and the reaction was initiated with 1 nM enzyme. For all assays with a 10-fold increase in β-lactamase, inhibitor and 10 nM enzyme were incubated for 5 min, and the reaction was initiated with 100 μM cephalothin-G-ester, the C3′ methyl ester of the cephalothin analogue bearing the penicillin G side chain rather than the thiophene acetamide side chain. Cephalothin-G-ester was used because it was a slower substrate for the enzyme and allowed for the measurement of reaction rate over a 5 min interval, even with a 10-fold increase in enzyme concentration. Hydrolysis was monitored at 265 nm for cephalothin and cephalothin-G-ester and at 482 nm for nitrocefin.

For chymotrypsin assays, inhibitor and 28 nM enzyme were incubated for five minutes, and the reaction was initiated with 400 μM BTEE[26] or 200 μM succinyl-ala-ala-pro-phe-*p*-nitroanilide. Reaction progress was monitored at 260 nm for BTEE or 410 nm for succinyl-ala-ala-pro-phe-*p*-nitroanilide. For DHFR assays, inhibitor and 120 nM enzyme were incubated for five minutes, and the reaction was initiated with 100 μM NADPH and 100 μM DHF;[37] progress was monitored at 340 nm. For β-galactosidase assays, inhibitor and 4 nM enzyme were incubated for 5 min, and the reaction was initiated with 1 mM ONPG; hydrolysis was monitored at 420 nm. β-Galactosidase incubations and reactions were performed at 37 °C.

When used, BSA, guanidinium HCl, or urea was present at 0.1 mg/mL, 0.6 M, or 1 M, respectively, and incubated with enzyme and inhibitor before addition of substrate. The concentrations of guanidinium and urea were well below the C_m values for AmpC β-lactamase.[38]

Dialysis of Inhibitor and Enzyme. Inhibitor at 20 times the IC_{50} or DMSO alone was incubated with 10 nM β-lactamase in 10 kDa dialysis tubing. Ten milliliters of this solution was dialyzed at room temperature against three 1 L volumes of 50 mM KP_i buffer, pH 7.0, exchanged hourly. After dialysis, the incubation solution was diluted 10-fold and assayed for β-lactamase activity against 100 μM cephalothin.

Dynamic Light Scattering (DLS). Compounds were generally dissolved to 10 mM in DMSO and diluted with filtered 5, 50, or 500 mM KP_i. Most compounds were analyzed with a 3 W argon-ion laser at 514.4 nm with BI-9000 and BI-200 optical systems from Brookhaven Instrument Corporation. The laser power and integration times were comparable for all experiments on this instrument. Calculation of mean particle diameter was performed by the cumulant analysis tool of a 400-channel BI9000AT digital autocorrelator, with the last eight channels used for baseline calculation. Congo Red and Rose Bengal lactone absorb light at 514.4 nm and therefore were analyzed with a Beckman-Coulter N4 Plus particle analyzer with a 10 mW helium−neon laser at 632.8 nm; particle size was calculated with the SDP analysis tool included by the manufacturer. For both instruments, the detector angle was 90°. Each diameter and intensity value represents four or more independent measurements at 25 °C.

Transmission Electron Microscopy (TEM). Solutions of 100 μM tetraiodophenolphthalein, 50 μM Congo Red, or 625 μM ANS were prepared in 20 mM Tris, pH 7.2. At room temperature, 3 μL of each was applied to a carbon-coated grid and negatively stained with 1% uranyl acetate. Images were obtained with a Philips CM12 transmission electron microscope at 120 kV. Micrographs were recorded at 22000× magnification and 2 μm underfocus.

Supporting Information Available: The structures of the compounds shown in Tables 1 and 6 (except tris(dicarboxymethylene)fullerene-C3) have been deposited in .sdf format. This material is available free of charge via the Internet at http://pubs.acs.org.

Acknowledgment. We thank T. Doman, G. Maggiora, and Pharmacia for providing us with screening compounds; the Keck Biophysics Facility at Northwestern University; P. Messersmith; B. Beadle and R. Powers for β-lactamase expression; and J. Widom, A. Gross, and lab members for reading this manuscript. This work was supported by Grant GM59957 (to B.K.S.) from the National Institutes of Health. S.L.M. was partly supported by NIH T32-GMO8152 and a PhRMA Foundation Medical Student Fellowship.

References

(1) Kenny, B. A.; Bushfield, M.; Parry-Smith, D. J.; Fogarty, S.; Treherne, J. M. The application of high-throughput screening to novel lead discovery. *Prog. Drug. Res.* **1998**, *51*, 245−269.
(2) Broach, J. R.; Thorner, J. High-throughput screening for drug discovery. *Nature* **1996**, *384*, 14−16.
(3) Kuntz, I. D. Structure-based strategies for drug design and discovery. *Science* **1992**, *257*, 1078−1082.
(4) Walters, W. P.; Stahl, M. T.; Murcko, M. A. Virtual Screening − An Overview. *Drug Discovery Today* **1998**, *3*, 160−178.
(5) Schevitz, R. W.; Bach, N. J.; Carlson, D. G.; Chirgadze, N. Y.; Clawson, D. K.; Dillard, R. D.; Draheim, S. E.; Hartley, L. W.; Jones, N. D.; Mihelich, E. D.; et al. Structure-based design of the first potent and selective inhibitor of human non-pancreatic secretory phospholipase A2. *Nat. Struct. Biol.* **1995**, *2*, 458−465.
(6) Dunten, P.; Kammlott, U.; Crowther, R.; Levin, W.; Foley, L. H.; Wang, P.; Palermo, R. X-ray structure of a novel matrix metalloproteinase inhibitor complexed to stromelysin. *Protein Sci.* **2001**, *10*, 923−926.
(7) DesJarlais, R. L.; Seibel, G. L.; Kuntz, I. D.; Furth, P. S.; Alvarez, J. C.; Ortiz de Montellano, P. R.; DeCamp, D. L.; Babe, L. M.; Craik, C. S. Structure-based design of nonpeptide inhibitors specific for the human immunodeficiency virus 1 protease. *Proc. Natl. Acad. Sci. U.S.A.* **1990**, *87*, 6644−6648.
(8) Shoichet, B. K.; Stroud, R. M.; Santi, D. V.; Kuntz, I. D.; Perry, K. M. Structure-based discovery of inhibitors of thymidylate synthase. *Science* **1993**, *259*, 1445−1450.
(9) Sun, L.; Tran, N.; Tang, F.; App, H.; Hirth, P.; McMahon, G.; Tang, C. Synthesis and biological evaluations of 3-substituted indolin-2-ones: a novel class of tyrosine kinase inhibitors that exhibit selectivity toward particular receptor tyrosine kinases. *J. Med. Chem.* **1998**, *41*, 2588−2603.
(10) Boehm, H. J.; Boehringer, M.; Bur, D.; Gmuender, H.; Huber, W.; Klaus, W.; Kostrewa, D.; Kuehne, H.; Luebbers, T.; Meunier-Keller, N.; Mueller, F. Novel inhibitors of DNA gyrase: 3D structure based biased needle screening, hit validation by biophysical methods, and 3D guided optimization. A promising alternative to random screening. *J. Med. Chem.* **2000**, *43*, 2664−2674.
(11) Muegge, I.; Heald, S. L.; Brittelli, D. Simple selection criteria for drug-like chemical matter. *J. Med. Chem.* **2001**, *44*, 1841−1846.
(12) Lipinski, C. A.; Lombardo, F.; Dominy, B. W.; Feeney, P. J. Experimental and computational approaches to estimate solubility and permeability in drug discovery and development settings. *Adv. Drug. Delivery Rev.* **1997**, *23*, 3−25.
(13) Walters, W. P.; Ajay; Murcko, M. A. Recognizing molecules with drug-like properties. *Curr. Opin. Chem. Biol.* **1999**, *3*, 384−387.

(14) Ring, C. S.; Sun, E.; McKerrow, J. H.; Lee, G. K.; Rosenthal, P. J.; Kuntz, I. D.; Cohen, F. E. Structure-based inhibitor design by using protein models for the development of antiparasitic agents. *Proc. Natl. Acad. Sci. U.S.A.* **1993**, *90*, 3583−3587.
(15) Gschwend, D. A.; Sirawaraporn, W.; Santi, D. V.; Kuntz, I. D. Specificity in structure-based drug design: identification of a novel, selective inhibitor of *Pneumocystis carinii* dihydrofolate reductase. *Proteins* **1997**, *29*, 59−67.
(16) Filikov, A. V.; Mohan, V.; Vickers, T. A.; Griffey, R. H.; Cook, P. D.; Abagyan, R. A.; James, T. L. Identification of ligands for RNA targets via structure-based virtual screening: HIV-1 TAR. *J. Comput.-Aided Mol. Des.* **2000**, *14*, 593−610.
(17) Hopkins, S. C.; Vale, R. D.; Kuntz, I. D. Inhibitors of kinesin activity from structure-based computer screening. *Biochemistry* **2000**, *39*, 2805−2814.
(18) Schlein, M.; Ludvigsen, S.; Olsen, H. B.; Andersen, A. S.; Danielsen, G. M.; Kaarsholm, N. C. Properties of small molecules affecting insulin receptor function. *Biochemistry* **2001**, *40*, 13520−13528.
(19) Perola, E.; Xu, K.; Kollmeyer, T. M.; Kaufmann, S. H.; Prendergast, F. G.; Pang, Y. P. Successful virtual screening of a chemical database for farnesyltransferase inhibitor leads. *J. Med. Chem.* **2000**, *43*, 401−408.
(20) Rudyk, H.; Vasiljevic, S.; Hennion, R. M.; Birkett, C. R.; Hope, J.; Gilbert, I. H. Screening Congo Red and its analogues for their ability to prevent the formation of PrP-res in scrapie-infected cells. *J. Gen. Virol.* **2000**, *81 Pt 4*, 1155−1164.
(21) Joubert, F.; Neitz, A. W. H.; Louw, A. I. Structure-based inhibitor screening: A family of sulfonated dye inhibitors for malaria parasite triosephosphate isomerase. *Proteins* **2001**, *45*, 136−143.
(22) Wolff, D. J.; Papoiu, A. D.; Mialkowski, K.; Richardson, C. F.; Schuster, D. I.; Wilson, S. R. Inhibition of nitric oxide synthase isoforms by tris-malonyl-C(60)- fullerene adducts. *Arch. Biochem. Biophys.* **2000**, *378*, 216−223.
(23) Matter, W. F.; Brown, R. F.; Vlahos, C. J. The inhibition of phosphatidylinositol 3-kinase by quercetin and analogues. *Biochem. Biophys. Res. Commun.* **1992**, *186*, 624−631.
(24) Davies, S. P.; Reddy, H.; Caivano, M.; Cohen, P. Specificity and mechanism of action of some commonly used protein kinase inhibitors. *Biochem. J.* **2000**, *351*, 95−105.
(25) Fesen, M. R.; Kohn, K. W.; Leteurtre, F.; Pommier, Y. Inhibitors of human immunodeficiency virus integrase. *Proc. Natl. Acad. Sci. U.S.A.* **1993**, *90*, 2399−2403.
(26) Weston, G. S.; Blazquez, J.; Baquero, F.; Shoichet, B. K. Structure-based enhancement of boronic acid-based inhibitors of AmpC beta-lactamase. *J. Med. Chem.* **1998**, *41*, 4577−4586.
(27) Rishton, G. M. Reactive compounds and in vitro false positives in HTS. *Drug Discovery Today* **1997**, *2*, 382−384.
(28) Patera, A.; Blaszczak, L. C.; Shoichet, B. K. Crystal structures of substrate and inhibitor complexes with AmpC β-lactamase: Possible implications for substrate-assisted catalysis. *J. Am. Chem. Soc.* **2000**, *122*, 10504−10512.
(29) Miller, D. W.; Dill, K. A. Ligand binding to proteins: the binding landscape model. *Protein Sci.* **1997**, *6*, 2166−2179.
(30) Stopa, B.; Gorny, M.; Konieczny, L.; Piekarska, B.; Rybarska, J.; Skowronek, M.; Roterman, I. Supramolecular ligands: monomer structure and protein ligation capability. *Biochimie* **1998**, *80*, 963−968.
(31) Tanford, C. *The hydrophobic effect: formation of micelles and biological membranes*, 2d ed.; Wiley: New York, 1980; ix, 233.
(32) Cassell, A. M.; Asplund, C. L.; Tour, J. M. Self-assembling supramolecular nanostructures from a C60 derivative: nanorods and vesicles. *Angew. Chem., Int. Ed.* **1999**, *38*, 2403−2405.
(33) Skowronek, M.; Stopa, B.; Konieczny, L.; Rybarska, J.; Piekarska, B.; Szneler, E.; Bakalarski, G.; Roterman, I. Self-assembly of Congo Red- - A theoretical and experimental approach to identify its supramolecular organization in water and salt solutions. *Biopolymers* **1998**, *46*, 267−281.
(34) Auweter, H.; Haberkorn, H.; Heckman, W.; Horn, D.; Luddecke, E.; Rieger, J.; Weiss, H. Supramolecular structure of precipitated nanosize β-carotene particles. *Angew. Chem., Int. Ed.* **1999**, *38*, 2188−2191.
(35) Powers, R. A.; Blazquez, J.; Weston, G. S.; Morosini, M. I.; Baquero, F.; Shoichet, B. K. The complexed structure and antimicrobial activity of a non-beta-lactam inhibitor of AmpC beta-lactamase. *Protein Sci.* **1999**, *8*, 2330−2337.
(36) Lorber, D. M.; Shoichet, B. K. Flexible ligand docking using conformational ensembles. *Protein Sci.* **1998**, *7*, 938−950.
(37) Su, A. I.; Lorber, D. M.; Weston, G. S.; Baase, W. A.; Matthews, B. W.; Shoichet, B. K. Docking molecules by families to increase the diversity of hits in database screens: computational strategy and experimental evaluation. *Proteins* **2001**, *42*, 279−293.
(38) Beadle, B. M.; McGovern, S. L.; Patera, A.; Shoichet, B. K. Functional analyses of AmpC beta-lactamase through differential stability. *Protein Sci.* **1999**, *8*, 1816−1824.

JM010533Y